Please quote this SOP in your Methods.

Evaluation of Muscles by Magnetic Resonance Imaging (MRI)

SOP (ID) Number	DMD_D.2.2.004
Version	4.0
Issued	November 14th, 2008
Last reviewed	June 30th, 2010; February 8 th, 2013; June 13th, 2015; June 15th, 2019
Author	Joe Kornegay College of Veterinary Medicine and Biomedical Sciences, Texas A&M University, College Station, TX USA
Working group members	Pierre Carlier (Institut de Myologie, Paris, France) Didier Bertoldi (Institut de Myologie, Paris, France) Stephane Blot (Veterinary School of Medicine, Maison Alfort, France) Jean Laurent Thibaud (Veterinary School of Medicine, Maison Alfort, France) Margot Coville (INSERM, Nantes)
SOP responsible	Joe Kornegay
Official reviewer	Pierre Carlier

TABLE OF CONTENTS

1. OBJECTIVE

The study of muscle diseases has evolved from a classical time in which a diagnosis was based on clinical and pathologic features, to a modern period when muscle biopsies were further characterized through histo- and cytochemical techniques, to the current era of molecular diagnosis. With the advent of sophisticated molecular techniques, DMD can be diagnosed non-invasively without the need for muscle biopsy. As a result, baseline and follow-up pathologic data are not typically available to assess disease progression or response to therapy. Other surrogate biomarkers must be utilized to ensure that results of treatment trials are interpreted appropriately.

2. SCOPE AND APPLICABILITY

Most DMD natural history studies have included measurements of muscle strength, joint contractures, and timed function tests. Results from these tests are used to track disease progression and offer insight on clinical milestones, such as the loss of ambulation and the need for ventilatory support. Magnetic resonance imaging (MRI) has been used increasingly to provide meaningful data on the natural history and response to therapy of a number of diseases, including DMD.[1-6] Studies have also been done in golden retriever muscular dystrophy (GRMD)[7-13] and other canine dystrophinopathies.[14,15]

3. CAUTIONS

Dogs must be anesthetized. A magnetic resonance imaging unit is required. See METHODS and EVALUATION AND INTERPRETATION OF RESULTS (below) for guidance on interpretation.

4. MATERIALS

Separate personnel are utilized for anesthetic management, the imaging procedure, and image analysis. The imaging procedure was first done with a Siemens 3 Tesla (T) Allegra Head-only System and subsequently with a 3 T Siemens MAGNETOM Trio with Tim Whole Body System, both available through the University of North Carolina-Chapel Hill (UNC-CH) Biomedical Research Imaging Center. Dogs are now imaged with a 3T Siemens Verio MRI unit at Texas A&M. Our animal imaging protocol **(Table 1)** was originally based on one used previously in DMD patients at UNC-CH (Fan J, Howard J, and Lin W, unpublished observations) and has subsequently been modified (see 5.3 and reference 16 for details). This protocol provides excellent anatomic resolution, thus allowing region-of-interest measurements of MRI parameters. Image analysis has been done through the UNC Neuro Image Research and Analysis Laboratories (NIRAL) using the software program ITK-SNAP (http://www.itksnap.org)[17] and Insight Segmentation and Registration Toolkit (ITK, http://www.itk.org), which provides semi-automatic segmentation of medical images by using image interpolation methods, manual delineation, and image navigation. We have focused on the proximal pelvic limb.

Table 1. Pulse Sequences Used in GRMD MRI									
	TR (ms)	TE (ms)	FOV (mm)	Thickness (mm)	#Slices	Matrix	Orientation	Time	Resolution (mm)
T2w	3,000	406-409	256	1	160	256x256	transverse	16'38"	1X1X1
T2fs	3,000	406-409	256	1	160	256x256	transverse	16'38"	1X1X1
T2 Value #1	3,040	7-70; Δ7	256	2	200	256x256	transverse	7'10"	1X1X2
T2 Value #2	3,170	20-100; Δ20	230	7	300	256x256	transverse	7'28"	1X1X7
PD	200	2.43, 8.49, 12.13, 15.77	256	5	16	256x256	transverse	9'18"	1x1x5

TR = Repetition time; TE = Echo time; FOV = Field of View; T_2w = T2-weighted; T_2fs = T2-weighted fat-suppressed; PD = Point Dixon.

5. METHODS

5.1. Anesthetic protocol

20-30 minutes prior to anesthesia induction:

- Pre-anesthetic agents:
  - Atropine sulfate (0.04 mg/kg, IM)
  - Acepromazine maleate (0.02 mg/kg, IM) for dogs weighing greater than 5 kg
  - Butorphanol tartrate (0.4 mg/kg, IM)

Anesthetic induction:

- Anesthetic agents:
  - Propofol (up to 3 mg/kg, IV – slowly!) for dogs weighing greater than 5 kg
  - Isoflurane or sevoflurane (to effect, inhaled) (avoid masking down)

Anesthetic monitoring:

During anesthesia, ECG, heart and respiratory rate, blood pressure, end tidal (Et)CO_2, and saturation of hemoglobin by peripheral oxygen (SpO_2) are monitored continuously with a pulse oximeter (Cardell Multiparameter Monitor 9405, Minrad International, Inc, Orchard Park, NY). These values, as well as capillary refill time and anesthetic setting, are recorded every 15 minutes.

Anesthetic recovery:

Monitor affected and carrier dogs closely during anesthetic recovery until fully awake and in sternal recumbency.

- Naloxone (up to 0.4 mg/kg, SQ) for rapid recovery; given in ½ dose increments (1st dose given while the dog is still intubated and breathing O_2; 2nd dose, if necessary, after extubated and/or if respiration drops below 7 breaths per minute).

5.2. Position the dog in ventral recumbence, with the pelvic limbs extended caudally into the gradient coil (gradient strength 40mT/m) within the MRI gantry **(Figure 1)**. Care should be taken to position the limbs symmetrically so as to facilitate side-to-side comparison of the images. Note, in the case of inevitable asymmetry, MRI image software can be used to align the limb in 3-D planes.

Figure 1. Anesthetized dog positioned in sternal recumbence with the pelvic limbs in the MRI coil/gantry.

5.3. T_2-weighted image sequences without (T_2w) and with fat saturation (T_2fs) are acquired using a variable-flip-angle turbo spin echo (TSE) sequence. The time between the excitation pulse and the center of k-space is 400 ms. Importantly, the contrast is not determined only by the TE (400 ms), but also by the flip angle evolution scheme. Although a traditional TSE sequence would have very little signal at 400 ms, the variable flip angle sequence is similar in principle to hyper-echo. The hyper-echo reduces the specific absorption rate (SAR), while the variable flip angle sequence allows long TE times.[18,19] A multi-spin-echo T2 (MSE-T_2), using a ten-echo Carr-Purcell-Meiboom-Gill sequence, is acquired to calculate the T2 value map. Analysis of the images is completed in three modules: muscle segmentation, pre-processing, and biomarker analysis. As a prerequisite, we first segment the major proximal pelvic limb muscles in the MRI images. All proximal pelvic limb muscles are segmented but only five slices at the mid-femur are analyzed and averaged.[12,16]

5.4. Images have been uploaded via a password-protected procedure to the NIRAL. Investigators have remote access to the datasets via encrypted secure shell log-in directly to the NIRAL file server. All datasets, as well as derived data computed as part of the processing procedure, are maintained on RAID 5 disk storage to protect against single disc failures. Data are backed up daily, with bi-weekly offsite storage of the backup tapes.

5.5. Image analysis has been done through the NIRAL using the software program ITK-SNAP (http://www.itksnap.org)[17] and Insight Segmentation and Registration Toolkit (ITK, http://www.itk.org). We initially manually segmented individual muscles of the proximal pelvic limb and averaged a total of five consecutive images at the level of the mid-femur. However, we have found that a relatively straightforward interpolation method provides data more respresentative of the entire muscle.[12,16]

6. EVALUATION AND INTERPRETATION OF RESULTS

Principal MRI changes in DMD include an increase in T2 and decrease in T1 relaxation times due to accumulation of fat in affected muscles and an associated increase in whole body fat and decrease in muscle mass. Objective grading systems,[20,21] and quantitation of parameters such as cross-sectional area, contractile vs. non-contractile tissue content,

transverse relaxation time, and lipid fraction allow data to be compared over the course of the disease.[3] Data have shown consistency across centers.[4] Moreover, results have correlated with those of clinical functional tests and may be even more sensitive in predicting disease progression.[5,20] MRI has also been used to monitor DMD disease progression in treatment trials.[22,23] MRI changes correlate with pathologic lesions.[24]

The potential role of MRI as a biomarker in GRMD has been reported in both natural history and preclinical treatment papers. In the first study, the thoracic limbs of 2-month-old GRMD dogs scanned at 4 T had an abnormally high T2-weighted/T1-weighted signal ratio, greater T2-weighted image heterogeneity, and more pronounced signal enhancement post-gadolinium contrast.[7] These same authors extended this work to assess distal muscles of both the pelvic and thoracic limbs at 2, 4, 6, and 9 months.[8] Standard and fat-saturated T1, T2, and proton density-weighted images, as well as gadolinium enhancement, were assessed. GRMD muscles were variably affected and, when compared with normal, had increased T1 and T2 values and more intense gadolinium enhancement. Consistent with our own findings (below), the differential between normal and GRMD findings did not progress significantly with age and there was minimal increase in fat signal. They then later conducted natural history studies of the GRMD diaphragm, demonstrating increased signal intensity and thickening that distinguished affected versus normal dogs.[9] An additional study by another group of 3-month-old GRMD dogs showed increased signal intensity on T2-weighted images in which the fat signal was suppressed, increased T2 values, and greater enhancement with gadolinium, all consistent with inflammation associated with early necrosis.[10]

We have assessed MRI in GRMD dogs both longitudinally and at single time points.[11-13] Consistent with prior studies, signal-intense lesions, presumably corresponding to fluid accumulation in necrotic lesions, have been seen on fat suppressed, T2-weighted images in younger dogs, while increased fat deposition has been seen at later ages **(Figure 2)**. The severity of these changes has varied among muscles. We have focused our studies on the 3-12 month age period, since this time frame has most commonly been used for preclinical studies by our group and others.[11] The principal parameters assessed have included muscle volumes, T2 mapping values, and several texture analysis features, including a first-order intensity histogram texture feature (entropy) and two high order run length matrix features (short run emphasis [SRE] and run length non-uniformity [RLN]).[12,13,16] These texture analysis features are assessed as potential markers of patchy lesions such as necrosis.[12,16,25,26] Based on the mathematical model, we refer to short run emphasis as the Small Lesion Index (SLI) and non- uniformity as the Heterogeneity Index (HI). Both SLI and HI use the run-length matrix method. Compared to histogram-based biomarkers that use intensity data only, the run-length matrix method also considers the spatial distribution and intensity of the voxels. A gray-level 'run' is defined as a set of consecutive voxels of similar intensity level in a given direction within a predefined similarity range. This is run in a 3-dimentional matrix and is intended to detect lumps of hyper-intensity in MRI.

In a natural history study, the proximal pelvic limbs of ten GRMD and eight normal dogs were scanned at 3, 6, and 9–12 months of age.[12] Several MRI imaging and texture analysis biomarkers were quantified in seven muscles. Almost all MRI biomarkers readily distinguished GRMD from control dogs; however, only selected biomarkers tracked with longitudinal disease progression. The biomarkers that performed best were full-length muscle volume and the HI texture analysis biomarker. The biceps femoris, semitendinosus and cranial sartorius muscles showed differential progression in GRMD versus control dogs. MRI features in GRMD dogs showed dynamic progression that was most pronounced over the 3- to 6-month period. Volumetric biomarkers and water map values correlated with histopathological features of necrosis/regeneration at 6-months.

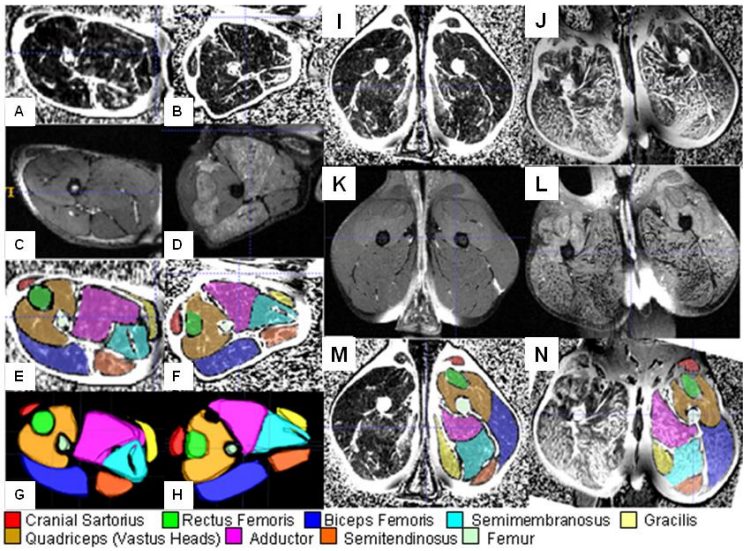

Figure 2. GRMD MRI Studies. The four panels from left to right are MRI images from a 2-month-old GRMD carrier (A,C,E,G) and affected littermate (B,D,F,H) and 5-year-old GRMD carrier (I,K,M) and affected dog (J,L,N). A, B, I, and J are TSE-fat percentage and C, D, K, and L are TSE-fat saturation. Transverse sections of muscle have been segmented in E, F, M, and N for region-of-interest measurements and are shown in three dimensions in G and H (2-month-old dogs only). Note, particularly, the signal-intense lesions in several muscles in D and J, representing fluid accumulation, acutely, and fatty change, chronically, respectively. Signal-intense lesions seen in J reverse with fat saturation in L. Segmentation was done using ITK-SNAP (http://www.itksnap.org/pmwiki/pmwiki.php).[17] From reference 11.

In the context of preclinical treatment trials, T2 signal was decreased in GRMD dogs treated systemically with morpholinos compared to age-matched untreated dogs, supporting a role for MRI as a biomarker in preclinical studies.[27] Another study showed that increased T2 signal could be used to track sites of AAV-micro-dystrophin construct injection.[28] Similarly, we have seen increased signal intensity in muscles associated with an apparent innate immune response in dogs treated with AAV-9 and a codon-optimized human mini-dystrophin.[29] More recently, T2w/T1w muscle signal ratios were normalized in GRMD dogs treated with AAV-micro-dystrophin via regional limb delivery.[30] Our lab demonstrated changes in texture features subsequent to treatment with a proprietary NF-κB inhibitor[13] and also showed differences in muscle cross sectional area and T2 map values in GRMD dogs bred to have reduced myostatin.[31] The myostatin study demonstrated correlation between certain functional and MRI indices. An analogous association between accelerometry and MRI indices has been shown in cross-bred GRMD dogs.[32]

Looking to the future, there is a great need for automated approaches for image analysis and, in tandem with this work, to further document that MRI biomarkers correlate with histopathologic changes. We have collaborated with engineers at Texas A&M to develop appropriate software programs.[33-35]

Potential Advantages/Disadvantages of the Methodology

Advantages

MRI is a non-invasive technique that can be used serially to quantitate end-points of both acute (edema) and chronic (fat deposition, volumetric changes) disease.

Disadvantages

Instrumentation and "scanner time" for sequential studies are expensive. There is considerable variation among MRI units and protocols, which could limit comparison of data. Results of MRI have not been correlated well with functional and pathologic studies.

7. REFERENCES

1. Finanger EL, Russman B, Forbes SC, Rooney WD, Walter GA, Vandenborne K: Use of skeletal muscle MRI in diagnosis and monitoring disease progression in Duchenne muscular dystrophy. Phys Med Rehabil Clin N Am. 2012 Feb;23(1):1-10, ix. doi: 10.1016/j.pmr.2011.11.004. Epub 2011 Dec 14.

2. Fischmann A, Hafner P, Gloor M, Schmid M, Klein A, Pohlman U, Waltz T, Gonzalez R, Haas T, Bieri O, Fischer D. Quantitative MRI and loss of free ambulation in Duchenne muscular dystrophy. J Neurol. 2013 Apr;260(4):969-74. doi: 10.1007/s00415-012-6733-x.

3. Akima H, Lott D, Senesac C, Deol J, Germain S, Arpan I, Bendixen R, Lee Sweeney H, Walter G, Vandenborne K: Relationships of thigh muscle contractile and non-contractile tissue with function, strength, and age in boys with Duchenne muscular dystrophy. Neuromuscul Disord. 2012 Jan;22(1):16-25. doi: 10.1016/j.nmd.2011.06.750. Epub 2011 Jul 31.

4. Forbes SC, Willcocks RJ, Triplett WT, Rooney WD, Lott DJ, Wang DJ, Pollaro J, Senesac CR, Daniels MJ, Finkel RS, Russman BS, Byrne BJ, Finanger EL, Tennekoon GI, Walter GA, Sweeney HL, Vandenborne K. Magnetic resonance imaging and spectroscopy assessment of lower extremity skeletal muscles in boys with Duchenne muscular dystrophy: a multicenter cross sectional study. PLoS One. 2014 Sep 9;9(9):e106435. doi: 10.1371/journal.pone.0106435. eCollection 2014. Erratum in: PLoS One. 2014;9(10):e111822.

5. Bonati U, Hafner P, Schädelin S, Schmid M, Naduvilekoot Devasia A, Schroeder J, Zuesli S, Pohlman U, Neuhaus C, Klein A, Sinnreich M, Haas T, Gloor M, Bieri O, Fischmann A, Fischer D. Quantitative muscle MRI: A powerful surrogate outcome measure in Duchenne muscular dystrophy. Neuromuscul Disord. 2015 Sep;25(9):679-85. doi: 10.1016/j.nmd.2015.05.006.

6. Burakiewicz J, Sinclair CDJ, Fischer D, Walter GA, Kan HE, Hollingsworth KG. Quantifying fat replacement of muscle by quantitative MRI in muscular dystrophy. J Neurol. 2017 Oct;264(10):2053-2067. doi: 10.1007/s00415-017-8547-3.

7. Thibaud J, Monnet A, Bertoldi D, Barthelemy I, Blot S, Carlier P: Characterization of dystrophic muscle in golden retriever muscular dystrophy dogs by nuclear magnetic resonance imaging. Neuromuscul Disord 17:575-584, 2007.

8. Thibaud JL, Azzabou N, Barthelemy I, Fleury S, Cabrol L, Blot S, Carlier PG: Comprehensive longitudinal characterization of canine muscular dystrophy by serial NMR imaging of GRMD dogs. Neuromuscul Disord. 2012 Oct 1;22 Suppl 2:S85-99.

9. Thibaud JL, Matot B, Barthélémy I, Fromes Y, Blot S, Carlier PG. Anatomical and mesoscopic characterization of the dystrophic diaphragm: An in vivo nuclear magnetic resonance imaging study in the Golden retriever muscular dystrophy dog. Neuromuscul Disord. 2017 Apr;27(4):315-325. doi: 10.1016/j.nmd.2017.02.003. Epub 2017 Feb 7.

10. Kobayashi M, Nakamura A, Hasegawa D, Fujita M, Orima H, Takeda S: Evaluation of dystrophic dog pathology by fat-suppressed T2-weighted imaging. Muscle Nerve 40:815-826, 2009.

11. Kornegay JN, Bogan JR, Bogan DJ, Childers MK, Li J, Nghiem P, Detwiler DA, Larsen CA, Grange RW, Bhavaraju-Sanka RK, Tou S, Keene BP, Howard JF, Jr, Wang J, Fan Z, Schatzberg SJ, Styner MA, Flanigan KM, Xiao X, Hoffman EP: Canine models of Duchenne muscular dystrophy and their use in therapeutic strategies. Mamm Genome 23:85-108, 2012.

12. Fan Z, Wang J, Ahn M, Shiloh-Malawsky Y, Chahin N, Elmore S, Bagnell CR, Jr, Wilber K, An H, Lin W, Zhu H, Styner M, Kornegay JN: Characteristics of magnetic resonance imaging biomarkers in a natural history study of golden retriever muscular dystrophy. *Neuromuscul Disord* 24:178-91, 2014.

13. Kornegay JN, Peterson JM, Bogan DJ, Kline W, Bogan JR, Dow JL, Fan Z, Wang J, Ahn M, Zhu H, Styner M, Guttridge DC. NBD delivery improves the disease phenotype of the golden retriever model of Duchenne muscular dystrophy. Skeletal Muscle 4:18, 2014.

14. Beltran E, Shelton GD, Guo LT, Dennis R, Sanchez-Masian D, Robinson D, De Risio L. Dystrophin-deficient muscular dystrophy in a Norfolk terrier. J Small Anim Pract. 2015 May;56(5):351-4. doi: 10.1111/jsap.12292. Epub 2014 Oct 29.

15. Jeandel A, Garosi LS, Davies L, Guo LT, Salgüero R, Shelton GD. J Small Anim Pract. 2018 Jan 29. doi: 10.1111/jsap.12824. [Epub ahead of print]

16. Wang J, Fan Z, Shiloh-Malawsky Y, An H, Kornegay JN, Styner M: A computerized MRI biomarker quantification scheme for a canine model of Duchenne muscular dystrophy. Int J Comput Assist Radiol Surg 8:763-774, 2013.

17. Yushkevich PA, Piven J, Hazlett HC, Smith RG, Ho S, Gee JC, Gerig G: User-guided 3D active contour segmentation of anatomical structures: significantly improved efficiency and reliability. Neuroimage 31:1116-28, 2006.

18. Hennig J, Weigel M, Scheffler K: Multiecho sequences with variable refocusing flip angles: optimization of signal behavior using smooth transitions between pseudo steady states (TRAPS). Magn Reson Med 49:527-535, 2003.

19. Hennig J, Speck O, Scheffler K: Optimization of signal behavior in the transition to driven equilibrium in steady-state free precession sequences. Magn Reson Med 48:801-809, 2002.

20. Liu GC, Jong Y-J, Chiang C-H, Jaw T-S: Duchenne muscular dystrophy: MR grading system with functional correlation. Radiology 186:475-480, 1993.

21. Chrzanowski SM, Baligand C, Willcocks RJ, Deol J, Schmalfuss I, Lott DJ, Daniels MJ, Senesac C, Walter GA, Vandenborne K. Multi-slice MRI reveals heterogeneity in disease distribution along the length of muscle in Duchenne muscular dystrophy. Acta Myol. 2017 Sep 1;36(3):151-162. eCollection 2017 Sep.

22. Arpan I, Willcocks RJ, Forbes SC, Finkel RS, Lott DJ, Rooney WD, Triplett WT, Senesac CR, Daniels MJ, Byrne BJ, Finanger EL, Russman BS, Wang DJ, Tennekoon GI, Walter GA, Sweeney HL, Vandenborne K. Examination of effects of corticosteroids on skeletal muscles of boys with DMD using MRI and MRS. Neurology. 2014 Sep 9;83(11):974-80. doi: 10.1212/WNL.0000000000000775. Epub 2014 Aug 6.

23. Hafner P, Bonati U, Erne B, Schmid M, Rubino D, Pohlman U, Peters T, Rutz E, Frank S, Neuhaus C, Deuster S, Gloor M, Bieri O, Fischmann A, Sinnreich M, Gueven N, Fischer D. Improved Muscle function in Duchenne muscular dystrophy through L-arginine and metformin: An Investigator-Initiated, open-label, single-center, proof-of-concept-study. PLoS One. 2016 Jan 22;11(1):e0147634. doi: 10.1371/journal.pone.0147634. eCollection 2016.

24. Kinali, M., Arechavala-Gomeza V, Cirak S, Glover A, Guglieri M, Feng L, Hollingsworth KG, Hunt D, Jungbluth H, Roper HP, Quinlivan RM, Gosalakkal JA, Jayawant S, Nadeau A, Hughes-Carre L, Manzur AY, Mercuri E, Morgan JE, Straub V, Bushby K, Sewry C, Rutherford M, Muntoni F: Muscle histology vs MRI in Duchenne muscular dystrophy. Neurology 76:346-53, 2011.

25. Herlidou S, Rolland Y, Bansard YL, Le Rumeur E, de Certaines JD: Comparison of automated and visual texture analysis in MRI: characterization of normal and diseased skeletal muscle. Magn Reson Imaging 17:1393-1397, 1999.

26. Mahmoud-Ghoneim D, Cherel Y, Lemaire L, de Certaines JD, Maniere A: Texture analysis of magnetic resonance images of rat muscles during atrophy and regeneration. Magn Reson Imaging 24:167-171, 2006.

27. Yokota T, Lu Q-L, Partridge T, Kobayashi M, Nakamura A, Takeda S, Hoffman E: Efficacy of systemic morpholino exon-skipping in Duchenne dystrophy dogs. Ann Neurol 65:667–676, 2009.

28. Wang Z, Storb R, Lee D, Kushmerick MJ, Chu B, Berger C, Arnett A, Allen J, Chamberlain JS, Riddell SR, Tapscott SJ: Immune responses to AAV in canine muscle monitored by cellular assays and noninvasive imaging. Mol Ther 18:617-24, 2010.

29. Kornegay JN, Li J, Bogan JR, Bogan DJ, Chen C, Zheng H, Wang B, Qiao C, Howard JF Jr, Xiao X: Widespread muscle expression of an AAV9 human mini-dystrophin vector after intravenous injection in neonatal dystrophin-deficient dogs. Mol Ther 18:1501-1508, 2010.

30. Le Guiner C, Servais L, Montus M, Larcher T, Fraysse B, Moullec S, Allais M, François V, Dutilleul M, Malerba A, Koo T, Thibaut JL, Matot B, Devaux M, Le Duff J, Deschamps JY, Barthelemy I, Blot S, Testault I, Wahbi K, Ederhy S, Martin S, Veron P, Georger C, Athanasopoulos T, Masurier C, Mingozzi F, Carlier P, Gjata B, Hogrel JY, Adjali O, Mavilio F, Voit T, Moullier P, Dickson G. Long-term microdystrophin gene therapy is effective in a canine model of Duchenne muscular dystrophy. Nat Commun. 2017 Jul 25;8:16105. doi: 10.1038/ncomms16105.

31. Kornegay JN, Bogan DJ, Bogan JR, Dow JL, Wang J, Fan Z, Liu N, Warsing LC, Grange RW, Ahn M, Balog-Alvarez CJ, Cotten SW, Willis MS, Brinkmeyer-Langford C, Zhu H, Palandra J, Morris CA, Styner MA, Wagner KR. Dystrophin-deficient dogs with reduced myostatin have unequal muscle growth and greater joint contractures. Skelet Muscle. 2016 Apr 4;6:14. doi: 10.1186/s13395-016-0085-7. eCollection 2016.

32. Kuraoka M, Nitahara-Kasahara Y, Tachimori H, Kato N, Shibasaki H, Shin A, Aoki Y, Kimura E, Takeda S. Accelerometric outcomes of motor function related to clinical evaluations and muscle involvement in dystrophic dogs. PLoS One. 2018 Dec 11;13(12):e0208415. doi: 10.1371/journal.pone.0208415. eCollection 2018.

33. Eresen A, McConnell S, Birch SM, Griffin JF, Kornegay JN, Ji JX. Localized MRI and histological image correlation in a canine model of Duchenne muscular dystrophy. Conf Proc IEEE Eng Med Biol Soc. 2016 Aug;2016:4083-4086. doi: 10.1109/EMBC.2016.7591624.

34. Eresen A, Birch SM, Alic L, Griffin Iv JF, Kornegay JN, Ji JX. New similarity metric for registration of MRI to histology: Golden retriever muscular dystrophy Imaging. IEEE Trans Biomed Eng. 2019 May;66(5):1222-1230. doi: 10.1109/TBME.2018.2870711. Epub 2018 Sep 17.

35. Eresen A, McConnell S, Birch SM, Griffin JF, Kornegay JN, Ji JX. Tissue classification in a canine model of Duchenne Muscular Dystrophy using quantitative MRI parameters. Conf Proc IEEE Eng Med Biol Soc. 2017 Jul;2017:4066-4069. doi: 10.1109/EMBC.2017.8037749.